Luma H. Abed

Department of Basic Sciences,
College of Dentistry,
University Al-Qadisiyah,
Al-Qadisiyah, IRAQ

Synthesis of Sb@Ge Core-Shell Nanostructures by Pulsed Laser Ablation in Water

Core-shell nanoparticles' structural, optical, and electrical features make them attractive medical and optoelectronic applications. Laser ablation in a liquid medium with a Nd:YAG laser (1064 nm, 480 mJ) produces Sb@Ge nanoparticles. Germanium (Ge) is the shell and antimony (Sb) the core. XRD, TEM, and AFM results indicate Sb@Ge cubic crystal structure with a 10 nm crystal size and core-shell shape. Ablation speeds crystallization and weakens particles. These results suggest Sb@Ge nanostructures could increase electrical and solar energy performance.

***Keywords*:** Nanoparticles; Core-shell structures; Antimony-Germanium alloy; Laser ablation
Received: 16 November 2024; **Revised:** 17 December; **Accepted:** 24 December 2024

1. Introduction

The synthesis of core-shell nanoparticles via laser ablation has garnered significant attention due to their unique properties and the flexibility of this fabrication method. This technique involves using an intense laser to vaporize a target material in a liquid medium, resulting in the formation of nanoparticles with a well-defined core-shell structure. These architectures exhibit distinct characteristics that enhance their applicability across various advanced technological fields [1].

This study focuses on the fabrication of Sb@Ge nanoparticles using the core-shell technique combined with pulsed laser ablation (PLA) [2]. Metallic nanoparticles, such as germanium (Ge) and antimony (Sb), possess unique nanoscale properties, including enhanced surface activity and tunable optical and electronic behavior. When synthesized via the core-shell method, these properties are further optimized, broadening their potential applications in cutting-edge technologies. Various fabrication approaches, including chemical and physical "top-down" methods, have been explored for producing such nanomaterials, each offering specific advantages in terms of precision and scalability [3,4].

A high-power pulsed laser is used to irradiate a target material in a liquid medium in this study to make core-shell nanoparticles [5,6]. A plasma plume is created by the contact, which is then cooled and condensed to make core nanoparticles. After that, a safe shell forms. The materials used are chosen to meet specific functional needs. These could be polymers, or materials coated on surfaces, alternative metals, or metal alloys [7, 8].

The core-shell method made it possible to make Sb@Ge nanoparticles that have amazing optical and structural features. An average particle size of 55 nm and a crystal size of 21 nm were seen in these nanoparticles. When compared to Sb and Ge nanoparticles made in the usual way, the synthesized Sb@Ge material had better qualities, nanoparticles are utilized in various physical applications, such as electronics and semiconductors, optics, thermoelectric energy generation, sensors, and battery performance enhancement. Their unique optical, electrical, and mechanical properties make them ideal for advanced technological innovations. such as better antibacterial activity [9].

This study shows that Sb@Ge core-shell nanoparticles could be useful in many areas, such as medicine, electronics, and catalysis. Additionally, the study shows that the core-shell method creates nanomaterials that are better than those made using more traditional methods [10-12].

The produced material demonstrates enhanced structural and optical properties, making it suitable for diverse physical applications, including medicine, electronics, and solar energy enhancement. This approach highlights the potential of advanced nanomaterials for innovative technological use

2. Experimental Part

This study primarily investigates the synthesis of Sb@Ge nanoparticles employing the core-shell technique through pulsed laser ablation

(PLA), as depicted in Fig. (1). For the preparation of the Sb target, 5 grams of Sb powder were compacted into a robust target using a five-ton press. The target was immersed in deionized water to support laser-induced nanoparticle generation. A neodymium-doped yttrium aluminum garnet (Nd: YAG) laser, operating at a wavelength of 1064 nm with a pulse energy of 480 mJ, was employed. The laser beam was focused with a 10 cm focal length lens, maintaining a 12 cm distance between the laser source and the Sb target.

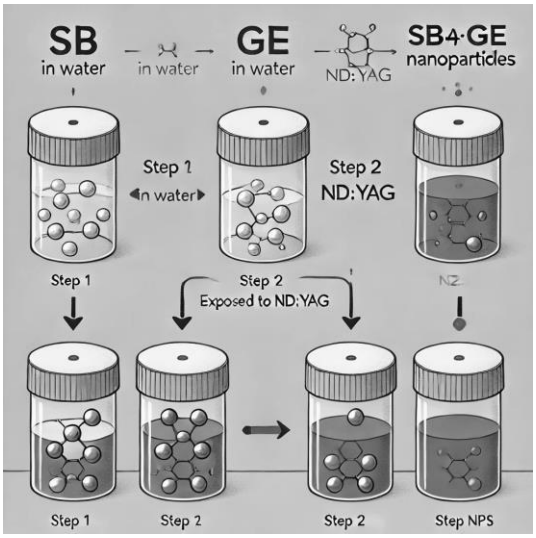

Fig. (1) The preparation process of Sb@Ge nanoparticles

During irradiation, a distinct color change in the liquid medium (Fig. 2) was observed, indicating nanoparticle formation. This optical transformation results from nanoscale phenomena, including localized surface plasmon resonance (LSPR), wherein collective oscillations of surface electrons in metallic nanoparticles selectively absorb specific light wavelengths, as well as quantum confinement effects that modify energy absorption and emission behaviors. Additionally, changes in light scattering properties and surface chemistry further confirm nanoparticle formation, highlighting variations in particle size, shape, and environmental interactions [13]. The laser ablation of Sb was conducted with a total of 700 pulses, ensuring efficient particle synthesis.

To ensure the successful formation of core-shell structures, 1000 laser pulses were applied to the Ge sample under precisely controlled conditions. These parameters were carefully optimized to achieve uniform and consistent deposition of the Ge layer onto Sb nanoparticles, as illustrated in Fig. (3). The plasmonic effect, triggered by the interaction of the laser with the nanostructures, significantly enhanced the chemical mobility of Ge atoms, promoting their effective encapsulation of Sb cores [13,14].

Fig. (2) Synthesis steps of Sb NPs

The methodology was meticulously regulated to ensure reproducibility and consistency across experiments. The Plasmon oscillations induced by the laser played a pivotal role in accelerating atomic diffusion and enhancing reaction kinetics, thereby facilitating the controlled growth of the core-shell architecture. This dynamic interaction underscores the critical influence of nanoscale plasmonic phenomena in achieving precise structural configurations.

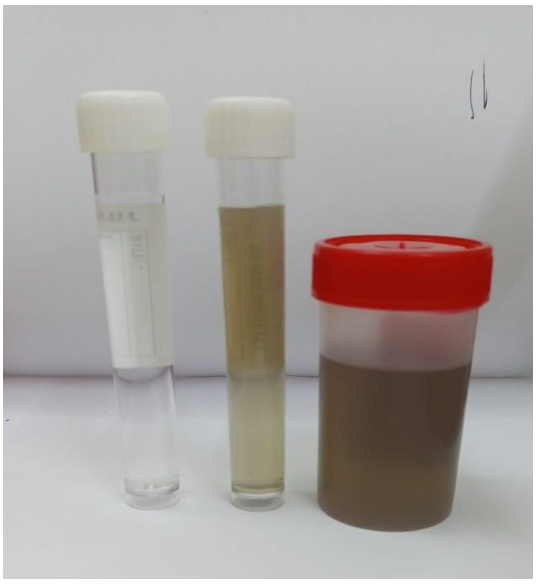

Fig. (3) Photograph of the Sb@Ge nanoparticles

3. Results and Discussion

X-ray diffraction is a crucial technique employed to determine the structure of crystals. It can be utilized to ascertain the atomic

arrangement, lattice parameters, strain, crystalline size, phase structure, and crystalline phases. This process led to the formation of a solid Sb phase encapsulated within Ge nanoparticles. To confirm the presence of the solid phase, X-ray diffraction (XRD) analysis was performed. The XRD measurements utilized Cu Kα radiation (wavelength 1.5418 Å) to capture diffraction patterns across a 2θ range of 10° to 80°, providing detailed insights into the crystal structure and composition of the synthesized nanoparticles [15]. Utilizing Cu Kα radiation within a 2θ range of 20° to 70° is optimal for capturing diffraction peaks essential for identifying Sb and Ge crystalline structures. Such parameters enhance the detection of phase compositions and minimize overlapping peaks, ensuring accurate structural analysis.

Figure (4) presents the X-ray diffraction (XRD) patterns of Sb@Ge core-shell nanoparticles, revealing two prominent peaks at 31.79° and 44.90°. These peaks correspond to the (111) planes of Sb and Ge, respectively, as indicated by the Ge JCPDS card number 04-0545. The presence of these peaks suggests a cubic crystal structure. The crystallite size, calculated using the Scherrer equation, is approximately 0.02 nm.The extremely small crystallite size (0.02 nm) suggested by the Scherer equation might indicate significant nanoscale defects or limitations in measurement resolution. Validation through complementary techniques, such as high-resolution TEM, is recommended to confirm such observations. Literature supports combining methods for enhanced reliability when assessing nanoscale structures [16].

The presence of Ge peaks in the diffraction pattern (JCPDS card No. 04-545) indicates that the Ge atoms have been safeguarded and transformed into core-shell nanoparticles of Sb @Ge [17, 18]. Figure 4 presents an X-ray diffraction (XRD) image illustrating that the synthesized nanoparticles (NPs) possess a core-shell nanostructure. Constructing a core-shell configuration facilitates the enhancement of crystallinity.

Core-shell configurations are widely recognized for improving material properties. For example, the Sb core in Sb@Ge nanoparticles may provide superior electronic characteristics, while the Ge shell enhances stability and resistance to oxidation, consistent with findings in other studies of core-shell nanomaterials.

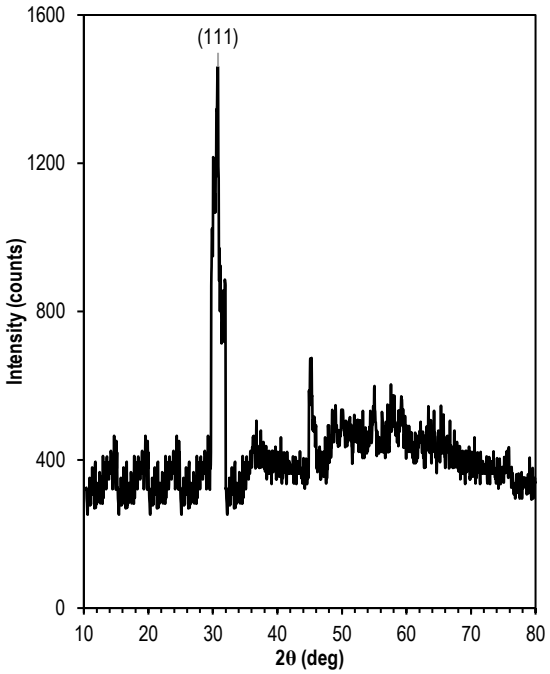

Fig. (4) XRD pattern of Sb@Ge core-shell nanoparticles prepared by pulsed laser ablation method

An atomic force microscope (AFM) picture of Sb @Ge nanoparticles made with pulse laser ablation and the core-shell method is shown in Fig. (5). There are Sb @Ge nanoparticles all over the top of the base, covering the whole thing. It is easy to see from the picture that the nanoparticles created with 480 mJ of laser energy are spread out evenly and are made up of small, smooth particles. Few single-pod rods are connected to these particles, which have a half-sphere shape with a tapered end. With the help of software, 9 nm was found to be the average particle size.

The uniform distribution of nanoparticles reflects effective laser ablation control. However, the formation of single-pod rods suggests potential non-uniformities during synthesis. Further optimization of energy and pulse duration could mitigate these effects, enhancing particle uniformity.

However, atomic force microscopy (AFM) only looks at the grain itself, not the size of the crystal defects. X-ray diffraction (XRD) measures the size-defect-free volume. Putting particles together is how bigger particles are made [19]. The root mean square method was used to figure out how rough the Sb @Ge particles' surface was. This test was done with a

laser that had 480 mJ of power. It was also found that the average sharpness was 3.21 nm and the average particle width was 9.2 nm. The root mean square (RMS) value is 2.221 nm, which is the average squared value of the surface heights and the standard deviation of the surface heights. A higher root mean square (RMS) number means that surface elevations change more.

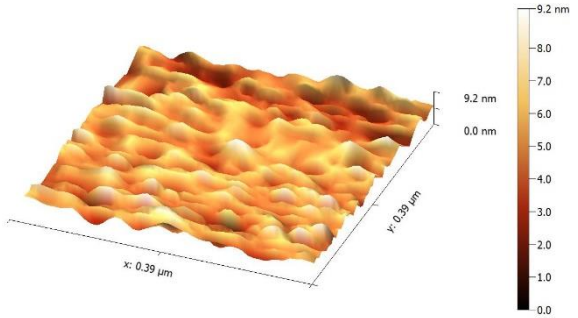

Fig. (5) 3D AFM image of Sb@Ge nanoparticles prepared by pulsed laser ablation

The RMS values indicate the degree of surface roughness, which is critical in applications like catalysis, where rough surfaces can enhance reactivity. Conversely, excessive roughness might negatively affect mechanical integrity or optical performance.

The square and average roughness is 3.512 nm, which is the average of the surface heights and shows how fast the surface is changing for the better. In addition, a second measurement of 9.2 nm is given, which shows the average size of the molecules or structures on the surface.

Transmission electron microscopy (TEM) was employed to examine the surface morphology of the fabricated samples, as illustrated in Fig. (6). Figure (6), together with the accompanying TEM images (7.01x7.83 inches; 512x572 pixels; 8-bit, 286k), demonstrates that the nanomaterial constitutes the core of the shell, as evidenced by the image. A circular substance is encircled by another circular material with varying concentrations. The inside ingredient is the core antimony (Sb), whereas the external substance is the shell germanium (Ge).

TEM images provide direct evidence of the core-shell structure, validating XRD findings. Such morphology confirms successful synthesis, with the core-shell design offering advantages like tailored optical properties and enhanced chemical resilience.

Figure (7) depicts the absorption spectra of Sb @Ge nanoparticles produced with a laser intensity of 480 mJ. Furthermore, according to the findings illustrated in Fig. (7), an increase in absorption is anticipated when the wavelength varies from 190 nm to 280 nm. A notable peak is observed at a wavelength of 210 nm. The transmittance of Sb@Ge nanoparticles, generated using laser light at 480 mJ, attains its minimum at a particular wavelength. Furthermore, the nanoparticles demonstrate a reduction in absorption beyond 210 nm, which is inconsistent with the transmittance behavior. The existence of these peaks is ascribed to the quantum size effect. Observations were conducted about the relationship between the intensity and width of Plasmon peaks and both the laser energy and the quantity of laser pulses [20,21].

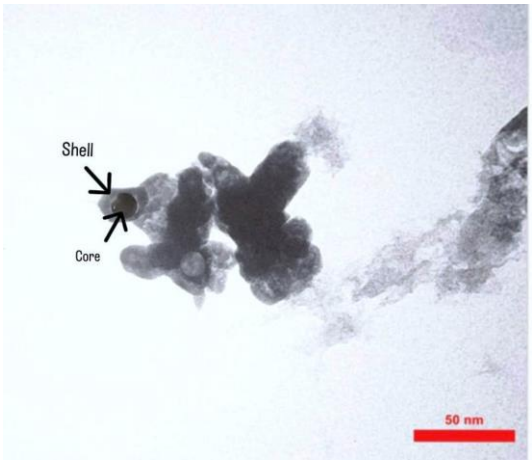

Fig. (6) TEM image of Sb@Ge core-shell nanoparticles prepared in this work

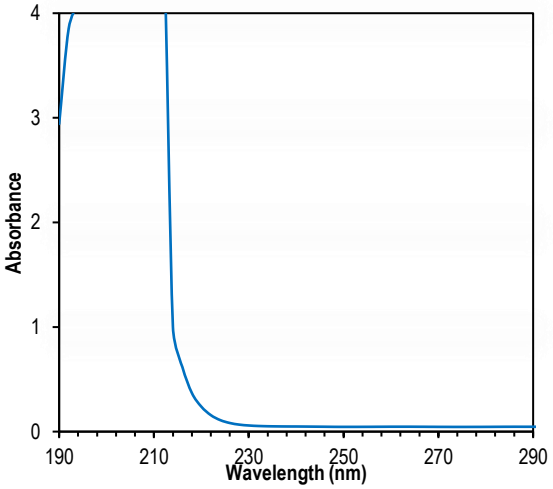

Fig. (7) UV-Visible absorption spectrum of Sb@Ge nanoparticles prepared in this work

The quantum size effect observed in the absorption spectra aligns with the nanoscale dimensions of the Sb@Ge particles. The peak at 210 nm likely corresponds to specific electronic transitions associated with the core-shell structure. Controlling Plasmon peaks through laser parameters can fine-tune optical properties, opening pathways for applications in photonics and sensing technologies [22].

4. Conclusion

The synthesized nanoparticles exhibit a well-defined cubic structure with highly agglomerated Sb@Ge core-shell structures. The nanoparticles display a unique multi-armed morphology, where spherical particles form funnel-like core-shell arrangements. These nanoparticles showed smooth surfaces and nanoscale precision. The results suggest that the Sb@Ge nanoparticles hold substantial potential for diverse applications, particularly in biomedicine and advanced material development, where precise structural control and exceptional surface characteristics are vital.

References

[1] B.A. Hasoon et al., "Promising antibiofilm formation: Liquid phase pulsed laser ablation synthesis of Graphene Oxide@Platinum core-shell nanoparticles", *PLOS ONE*, 19(9) (2024) e0310997.

[2] K. Chandra Bhowmik et al., "From Lithium-Ion to Sodium-Ion Batteries for Sustainable Energy Storage: A Comprehensive Review on Recent Research Advancements and Perspectives", *The Chem. Record*, 24(12) (2024) e202400176.

[3] M.Z. Ul Abidin et al., "A comprehensive review on the synthesis of ferrite nanomaterials via bottom-up and top-down approaches advantages, disadvantages, characterizations and computational insights", *Coordin. Chem. Rev.*, 520 (2024) 216158.

[4] N. Borane et al., "Recent trends in the "bottom-up" and "top down" techniques in the synthesis and fabrication of myriad carbonaceous nanomaterials", in **Carbon-Based Nanomaterials in Biosystems**, Academic Press (2024), pp. 91-120.

[5] H. Naderi-Samani and R.S. Razavi, "Synthesis of Nanoparticles Using Pulsed Laser", in Pulsed Laser Processing of Materials, D. Yang and K. Gibson (ed.), IntechOpen (2024), doi: 10.5772/intechopen.1004415.

[6] R. Walden et al., "Nonthermal plasma technologies for advanced functional material processing and current applications: Opportunities and challenges", *J. Enviro. Chem. Eng.*, 12(5) (2024) 113541.

[7] L. Yang et al., "Synthesis Strategies for High Entropy Nanoparticles", *Adv. Mater.*, (2024) 2412337, published online 30 October 2024.

[8] T.M. Rashid, U.M. Nayef and M.S. Jabir, "Synthesis of Au/ZnO nanocomposite and Au: ZnO core: shell via laser ablation for of photo-catalytic applications", *Mater. Technol.*, 37(13) (2022) 2457-2464.

[9] Y. Hou et al., "Fabrication of hierarchical Au@Fe_2O_3-SnO_2 core-shell nanotubes with high n-butanol sensing performance", *Sens. Actuat. B: Chem.*, 406 (2024) 135387.

[10] S. Bilge et al., "Recent trends in core/shell nanoparticles: their enzyme-based electrochemical biosensor applications", *Microchimica Acta*, 191(5) (2024) 240.

[11] D.R.S. Almeida et al., "Advances in Microfluidic-based Core@Shell Nanoparticles Fabrication for Cancer Applications", *Adv. Healthcare Mater.*, 13(23) (2024) 2400946.

[12] D. Zhen et al., "Developing core-shell silica nanoparticles to create multifunctional coating with excellent antireflection, enhanced antifogging and anticorrosion performances", *Prog. Org. Coat.*, 186 (2024) 107956.

[13] F.J. Kadhim, O.A. Hammadi and N.H. Mutesher, "Photocatalytic activity of TiO_2/SiO_2 nanocomposites synthesized by reactive magnetron sputtering technique", *J. Nanophot.*, 16(2) (2022) 026005.

[14] X. Jin et al., "*in situ* Surface Reconstruction in Pure Water by Ice-Confined Freeze-Thaw Strategy for High-Performance Core–Shell Structural Perovskite Nanocrystals", *Adv. Func. Mater.*, 34(28) (2024) 2401435.

[15] A.A. Arunmozhi et al., "Growth and characterization of novel Curcuma longa natural dye-doped sodium p-nitrophenolate dihydrate single crystals for nonlinear optical applications", *J. Mater. Sci.: Mater. Electron.*, 35(28) (2024) 1866.

[16] C. Jin et al., "Effect of crystallite size on lithium storage performance of high entropy oxide $(Cr_{0.2}Mn_{0.2}Co_{0.2}Ni_{0.2}Zn_{0.2})_3O_4$ nanoparticles", *Electrochimica Acta*, 506 (2024) 145004.

[17] J. Wang et al., "Amorphous germanium encapsulated in flexible nitrogen-doped carbon nanofiber for sodium storage with ultra-long cycling stability", *J. Colloid Interface Sci.*, 680B (2024) 437-445.

[18] M. Aouassa et al., "Growth of Ge QDs-Decorated SiGe Nanocrystals: Toward Integration of Quantum Dots and Mie Resonators in Ultrathin Film for Photodetection and Energy Harvesting",

ACS Appl. Electron. Mater., 6(5) (2024) 3290-3296.

[19] L.H.A. Anza and S.N. Abdulwahid, "Examining the Antimicrobial Capabilities and Methods for Preparing Core-Shell Laser-Synthesized CdS@ Cu Nanoparticles", *J. Kufa Univ. Phys.*, 16(01) (2024) 80-93.

[20] D. Mahmoud et al., "Laser Ablation of Tungsten Metal for Au@WO_3 Core-Shell Formation: A Characterizing Study at Different Laser Fluences", *Plasmonics*, (2024), doi: 10.1007/s11468-024-02607-8.

[21] L.H. Abed and S.N. Abdulwahid, "Fabrication and Characterization of Cadmium Sulfide Nanoparticles via Laser Ablation Method", *Iraqi J. Appl. Phys.*, 20(1) (2024) 111-116.

[22] K. Okamoto et al., "Design and Optimization of Silver Nanostructured Arrays in Plasmonic Metamaterials for Sensitive Imaging Applications", *Photonics*, 11(4) (2024) 292.

